Volume 1 | Number 1 | Jan 2013 | Pages 1–100

Soft Matter

www.rsc.org/softmatter

This is an *Accepted Manuscript*, which has been through the Royal Society of Chemistry peer review process and has been accepted for publication.

Accepted Manuscripts are published online shortly after acceptance, before technical editing, formatting and proof reading. Using this free service, authors can make their results available to the community, in citable form, before we publish the edited article. We will replace this *Accepted Manuscript* with the edited and formatted *Advance Article* as soon as it is available.

You can find more information about *Accepted Manuscripts* in the **Information for Authors**.

Please note that technical editing may introduce minor changes to the text and/or graphics, which may alter content. The journal's standard **Terms & Conditions** and the **Ethical guidelines** still apply. In no event shall the Royal Society of Chemistry be held responsible for any errors or omissions in this *Accepted Manuscript* or any consequences arising from the use of any information it contains.

www.rsc.org/softmatter

Soft Matter

ARTICLE

Micro-Viscosity of Liquid Oil Confined in Colloidal Fat Crystal Networks

H. Du[a], C. Kim[a], M.G. Corradini[a], R.D. Ludescher[a], and M.A. Rogers[a]

Molecular rotors may be utilized as non-invasive, non-disruptive and highly sensitive alternatives to conventional measures of bulk viscosity when the oil is entrained in a colloidal fat crystal network. Oil viscosity changes based on the molecular confinement of the oil, which is dependent on its molecular volume. Changes in micro-viscosity were not dependent on the solids content, but instead were strongly dependent on the box-counting fractal dimension in high-space filling colloidal fat crystal networks (i.e., D > 1.89). A bulk oil viscosity is often an overestimation of the actual viscosity of the entrained oil and may not be appropriate when predicting diffusion in multi-phase materials.

Introduction

Gels comprised of self-associating colloidal networks have unique applications as elastic biomaterials in foods,[1-3] medicine,[4] inks,[5] and pharmaceutical delivery agents.[6] The capacity of the network to entrap the continuous liquid phase directly influences stability, permeability and functionality.[7] This is of utmost importance in edible colloidal fat crystal networks, where the ability of the network to entrain the liquid component directly influences oil mobility.[7] For example, mobility of oil in chocolate-based products accelerates bloom and softening.[8-11] Although the macroscopic measurement of oil mobility in colloidal networks is relatively straightforward,[7, 12] the influence of the colloidal nature of the network on the confinement and hence viscosity of oil is not well understood.

Numerous mechanisms have been proposed for the driving force for oil migration, which arises based on either differences in liquid fat content or a gradient in triacylglycerol concentration.[12, 13] Using an unsteady state concentration gradient of one component as the driving force for diffusion, Fick's second law may be extended to:[13]

$$\frac{\delta c}{\delta t} = \frac{\delta}{\delta x}\left(D \frac{\delta c}{\delta x}\right) \tag{1}$$

where c is the concentration, t is time, x is the distance and D is the diffusivity. The diffusivity takes the following form:

$$D = -\frac{kT}{6\pi\eta r} \tag{2}$$

where k is Boltzman constant, T is the absolute temperature, η is the viscosity and r is the molecular radius of the diffusing particle. Irrespective of the underlying driving force and theory used to describe the mobility, in colloidal networks, a permeability coefficient, β, and viscosity, η, are often combined in the form of Darcy's Law:

$$Q = \frac{\beta A_c}{\eta} \times \frac{\Delta P}{L} \tag{3}$$

where Q is the volumetric flow rate, A_c is the cross sectional area, η is the viscosity of the liquid oil, and ΔP is the pressure drop over the distance, L. β is dependent on numerous structural characteristics including particle radius, a, a tortuosity factor, K, the solids content, ϕ, and the fractal dimension, D.[14]

$$\beta = \left(\frac{a^2}{K}\right) \phi^{2/(D-3)} \tag{4}$$

In general, the microstructural elements of colloidal fat crystal networks such as the particle size, tortuosity and fractal dimension may be accessed using simple techniques including: microscopy, rheology and/or light scattering techniques. However, the viscosity is not a measure of the macroscopic viscosity of the material but instead the viscosity of the entrained liquid oil, as this is the path of migration.[13] It is the objective of this manuscript to determine if the confinement of liquid oil in a colloidal fat crystal network alters the viscosity of the continuous phase using molecular rotors. The use of fluorescent molecular rotors can, in principle, enable the sensitive characterization of the microenvironment in fat crystal networks.

Molecular rotors define molecules that consist of two or more parts that can easily rotate relative to each other.[15, 16] Upon

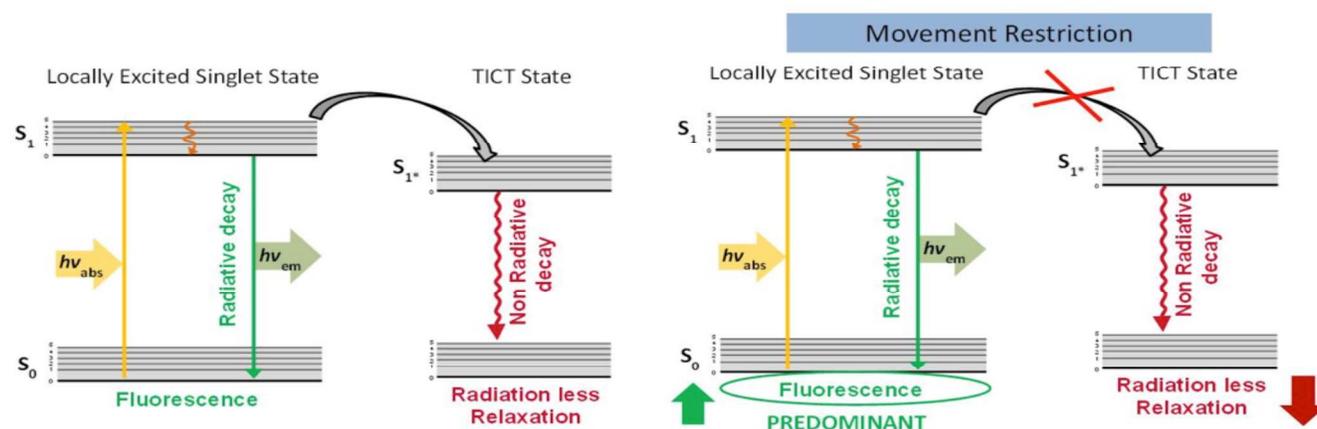photoexcitation these compounds can undergo twisted intra-

Figure 1. Jablonski diagram of a single emission band molecular rotor. Left- Notice that relaxation from the TICT state occurs without fluorescence emission. Right - Restriction of the twisted state increases fluorescence emission. Adapted from Haidekker and Theodorakis.[17]

molecular charge transfer (TICT) which is the rotation of one of the segments of the molecule relative to the other.[18] Deactivation from the TICT state occurs through a nonradiative pathway, and radiative decay, which results in emission of a photon, is observed from the locally excited state. These two competing relaxation pathways determine the sensitivity of the probe to the micro-viscosity of the surrounding environment since TICT state formation rate is lower in more viscous environments.[17, 19, 20] In a less viscous fluid environment the molecule undergoes fast internal rotation (Figure 1), and thus fast radiationless decay.[21] Environmental restrictions to intramolecular twisting result in an increase in fluorescence emission. Changes in emission properties of fluorescent molecular rotors (specifically, fluorescence quantum yield, intensity and lifetime) have been correlated to the local (or micro) and bulk viscosity of the medium,[22] polymerization and aggregation processes,[18] and phase transitions.[17]

Methods

Tristearin was used as the solid component and the liquid oil was either a medium-chain triglyceride oil (i.e., tricaproin, tricaprylin, and tricaprin) or an unsaturated oil (i.e., triolein and trilinolein) (Sigma Aldrich, St. Louis, MO, USA). Fat blends were prepared from 30 to 100 wt% tristearin at 10 wt% intervals in each liquid oil. The blends were heated to 80 °C, above the melting point of tristearin, and held for 20 min and then stored for 24 hrs in a 35 °C temperature controlled incubator before analysis.

Solid fat content
Samples were subjected to T_2 relaxation measurements on a Bruker mq20 Series NMR Analyzer (Bruker, Milton, Ontario, Canada). A Hahn-echo pulse sequence was used to measure the free induction decay (FID), T_2 relaxation of the solid crystalline component (< 70 μs) of the blends.[23, 24] The operational pulse length was obtained using the calibration procedures recommended by the manufacturer. The 90° pulse was 2.6 μs and the 180° pulse was 5.1 μs. This allowed determination of the gain (64) and recycle delay (5 sec). Tau was selected to be

as short as possible (0.5 ms) to minimize chemical exchange and diffusion effects on the decay curves.

Polarized light microscopy and fractal analysis
The supramolecular structure of the fat blends were imaged using a Linkham Imagining Station (Linkham, Surrey, England) equipped with a Q imagining 2560 x 1920 pixel CCD camera (Micropublisher, Surrey, Canada) and a 10 X Olympus lens (0.25 N.A.) (Olympus, Tokyo, Japan). Samples were placed on a glass slide and a cover slip was set on top of the sample. The slide was transferred into a Peltier temperature control stage (LTS120, Linkham, Surrey, England) using a water reservoir as the heat sink and imaged at 35 °C to observe crystal structure using non-polarized light. Light micrographs were calibrated with a 100 μm micrometer.

Using the polarized light micrographs, Image J (NIH, Bethesda, MD) was used to calculate a box-counting fractal dimension, D_f, using the fractal dimension and lacunarity, FracLac, plugin.[25] The box-counting algorithm is a simple method to quantify complex structures by laying successively sized grids over digital images and the foreground pixels (the crystal area) are counted in each box. Boxes must be completely void of crystals to be excluded. D_f is calculated using the relationship between the number of boxes containing crystals, N, and the size of the overlaying box, ε:

$$N \propto \varepsilon^{-D_f} \qquad (5)$$

Micro-viscosity
1-(2,5-dimethoxy-phenylazo)-naphthalen-2-ol (Citrus red 2 (CR)) was purchased from Sigma-Aldrich (St. Louis, MO, USA) and used without further purification. Stock solutions (1mM) of this food dye were prepared in DMSO, ethanol, ethylene-glycol 99% purity, glycerol (spectrophotometric quality – 99.5% purity), hexane and tricaprylin. The stock solutions were used to obtain CR excitation and emission spectra and to assess the viscosity and *polarity* sensitivity of CR's fluorescence intensity in solutions. DMSO, ethanol, hexane and polyols were obtained from Fisher Scientific (Pittsburgh, PA).

Fluorescence emission of Citrus red 2 in polar protic, polar aprotic and nonpolar solvent solutions

Since limited information on the photophysical properties of CR is available, stock solutions of CR were diluted to 10 uM to obtain the fluorescence excitation and emission spectra of the dye in protic, aprotic and nonpolar solvent solutions. Steady state fluorescence excitation and emission spectra were recorded using a Fluoromax-3 spectrofluorometer (Horiba Scientific Inc., Edison, NJ). 10 uM CR solutions were tested in 1 cm lightpath quartz cuvettes (NSG Precision Cells, Farmingdale, NY) at 35 °C. Preliminary runs were conducted to identify the optimal excitation wavelength and emission and excitation slits for each sample. The fluorescence emission intensity in counts per second, peak emission and excitation wavelength were determined. The effect of dye concentration on fluorescence intensity was further tested in order to minimize inner filter effect in subsequent studies.

Citrus red fluorescence emission in solutions of different viscosities

To assess CR sensitivity to viscosity, the fluorescence emission intensity of 10 uM solutions of CR in binary mixtures of ethylene glycol and glycerol was recorded using a Fluoromax-3. All measurements were performed at 35 °C. As reported in the literature [19, 26, 27] variations in viscosities within a 15-400 mPa s range can be obtained by modifying the ethylene glycol (low viscosity solvent)-glycerol (high viscosity solvent) ratio. The dependence of CR fluorescence intensity on the surrounding medium's viscosity was also assessed in pure glycerol whose viscosity was modified using temperature to attain values between 30-12000 mPa s.

The Förster and Hoffman equation relates the fluorescent quantum yield, Φ_F, of a molecular rotor to the viscosity (η) of the surrounding solution.[28] This relationship can be described as follows (Eq. 6):

$$\log \Phi_F = C + x \log \eta$$

(6)

where C and x are solvent and dye dependent constants.

Since fluorescence emission intensity, I_F, and quantum yield are proportional, the relationship between fluorescence intensity and viscosity can be reworked from Eq. 5 and expressed by the following power law model (Eq. 7):[17]

$$I_F = \alpha \eta^x$$

(7)

where α can be considered a measure of the probe's brightness and x a measure of its sensitivity to local viscosity.[27] The relationship between maximum fluorescence intensity and viscosity of the CR solutions was fitted using Eq. 7 and sensitivity of CR to viscosity (x) was compared to reported values of commonly used molecular rotors in similar systems. The applicability of Eq. 7 was also verified by the linear correspondence of fluorescence intensity and viscosity plotted in a double-logarithmic scale.

Evaluation of microenvironment in confined solid fat networks using Citrus red 2

Movement restriction of a molecular rotor, in this case CR, results in noticeable increase in fluorescence emission intensity. Based on this observation a spectrofluorometric technique was developed to characterize the microenvironment in solid fat networks. 10 mM CR stock solutions were prepared in five triacylglycerols, namely tricaproin, tricaprylin, tricaprin, triolein and trilinolein, all of which are liquid a room temperature. CR was embedded in the fat blends by partial substitution of the liquid oil solvent by the corresponding CR stock solution to attain a final concentration of the fluorescent dye of 0.85 mM. The concentration in the fat blends was higher than that used in solutions to account for the lack of clarity in the solid fat samples.

Once the fat blends were prepared with and without the addition of CR, they were heated up to completely melt the solid fat component. A 10 uL aliquot of each mixture was deposited on the center of custom-made quartz slides (10 mm x 25 mm, NSG Precision Cells). The slides were kept at 40 °C to facilitate dispensing of the complete volume and prevent solidification of the fat mixture upon contact with a cold surface. The dimensions of the sample were checked for consistency using a caliper. The samples were incubated at 35 °C for at least 24 hrs before testing. The slides were inserted at a 45° angle in a 1 cm light-path quartz cuvette. Their fluorescence emission spectra were recorded using a Fluoromax-3. On the emission end a 550 nm longpass cut-on filter was mounted to eliminate disturbances by scattered excitation light. The excitation wavelength and the excitation and emission slits were set at 540 nm and 3 nm, respectively. The fluorescence emission spectra were normalized and the blank subtracted from the corresponding CR spectra. All samples were run at least in triplicate.

Results and Discussions

Synthetic food colors are widespread in products due to their stability and functionality at low concentrations. 1-(2,5-dimethoxy-phenylazo)-naphthalen-2-ol (Citrus red 2 - CR) is a color additive normally applied to the surface of fresh oranges to enhance their external appearance. CR was selected based on its solubility (insoluble in water, soluble in organic solvents) and ready availability. Additionally, preliminary results indicated easy differentiation of the emission band of CR from background noise.

As seen in Fig. 2, Citrus red 2 contains one functional azo group. The presence of the azo group potentially confers molecular rotor properties to this dye such that it exhibits low fluorescence emission intensity in low viscosity fluid solutions and a significant enhancement of fluorescence intensity in highly viscous solvents. Abbott et al. [29] have studied the dynamics of excited states of azo dyes in solutions. Their estimations indicate that excited state tautomerization and/or internal twisting are likely to constitute the predominant nonradiative relaxation pathway in azo dyes in low viscosity solutions.
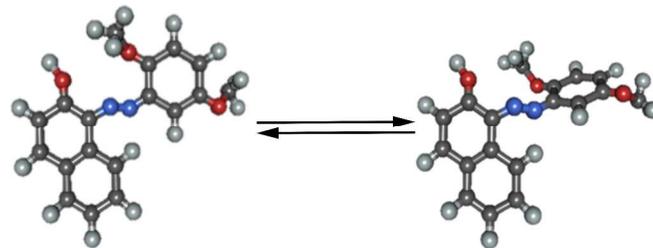

Figure 2. Structure and possible intramolecular rotation in Citrus Red 2.

Emission and excitation spectra of CR in polar protic (ethanol, ethylene glycol and glycerol) solutions and emission spectra as a function of polarity are shown in Fig. 3 A and B, respectively. The data were normalized toards CR in glycerol to illustrate the effect of the surrounding viscosity on the fluorescence intensity of CR. As can be observed in Fig 3, CR is practically non emissive in common solvents, which can explain the limited information on its photophysical properties.
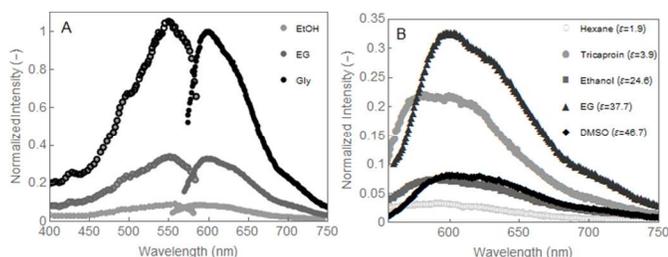

Figure 3. A- Excitation (empty circles) and emission (solid circles) spectra of CR in solvents of similar polarity and different viscosity. B- Effect of polarity on the emission spectra of CR. Permittivity (ε) of solvents is reported between brackets.

CR's Stokes shift, (ℓ_{em}-ℓ_{exc}), was estimated to be 45-60 nm depending on the medium. Environmental polarity only moderately impacted the location of the peaks and, consequently, Stokes shift. Although a bathochromic shift was observed as the polarity of the solvents increased, the magnitude of the shift (~15 nm) was equivalent to that of other commonly reported molecular rotors in similar environments, for example, 9-(2,2-dicyanovinyl)-julolidine (DCVJ).[30]

The sensitivity of CR fluorescence emission intensity to the medium's rigidity, evaluated as viscosity of the surrounding media, is shown in Figs. 4 and 5. To facilitate comparison within each experiment, the data were normalized so that the emission from the highest viscosity corresponds to unity. The maximum fluorescence intensity of CR increases as the viscosity of the surrounding media increases, regardless if the change in viscosity was temperature or concentration driven. Although the data were plotted in double logarithmic coordinates to verify the applicability of Eq. 7, the parameters of the power law relationship were obtained using a nonlinear regression procedure to minimize bias in the estimation.[31]
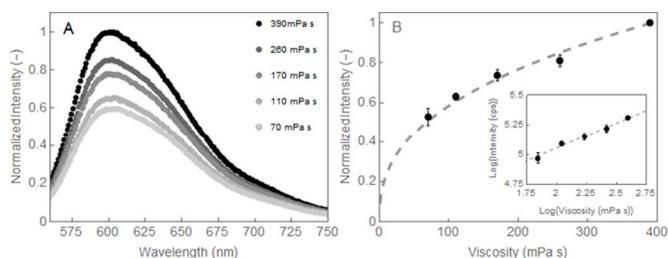

Figure 4. (A) Emission spectra of CR in ethylene glycol and glycerol mixtures. (B) Dependence of CR fluorescence intensity on viscosity fitted with Eq. 7. Inset: Relationship presented as a log-log plot.

While the maximum theoretical viscosity sensitivity of molecular rotors has been estimated to be 0.66, sensitivity values (x) of novel and commonly used molecular rotors have been reported in the range of 0.25 to 0.6 (i.e., 0.26-0.4 for

modified nucleosides,[32] 0.53 for DCVJ, 0.52 for 9-(2-carboxy-2-cyano)vinyl julolidine (CCVJ)[30] and 2-cyano-3-(4-dimethylaminophenyl) acrylic acid methyl ester (CMAM).[33] In the case of CR, the viscosity sensitivity was established to be 0.43, within the range reported for other molecular rotors.
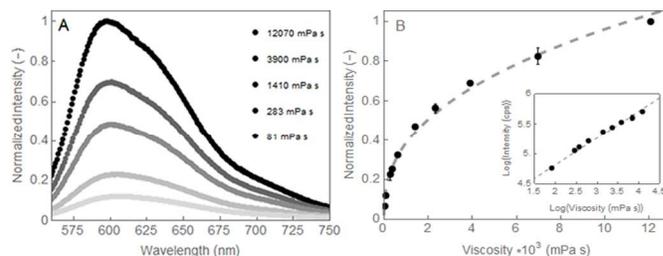

Figure 5. (A) Emission spectra of CR in glycerol at different temperatures. (B) Dependence of CR fluorescence intensity on viscosity fitted with Eq. 7. Inset: Relationship presented as a log-log plot.

A large Stokes shift and high sensitive to viscosity (or molecular rigidity) changes are two requirements of an adequate molecular rotor.[27] In principle, the behaviour of CR in relation to these two conditions, which is comparable that of other commonly used or recently proposed molecular rotors, establishes CR's molecular rotor character and supports its potential use as a probe of micro-viscosity or molecular crowding in solid fat networks. It should be also noticed that when CR was incorporated in solid fat samples, in contrast to reference samples stained with DCVJ, the location of its emission peak at about 600 nm and its Stokes shift facilitated differentiation from background noise. Examples of the emission spectra of CR in a solid fat crystal network of a saturated medium chain TAG (A) or an unsaturated long chain TAG (B) and tristearin are presented in Fig. 6. The shown emission spectra were obtained by subtracting the background spectra of each respective dye-free controls and correcting for scattering and dye concentration.
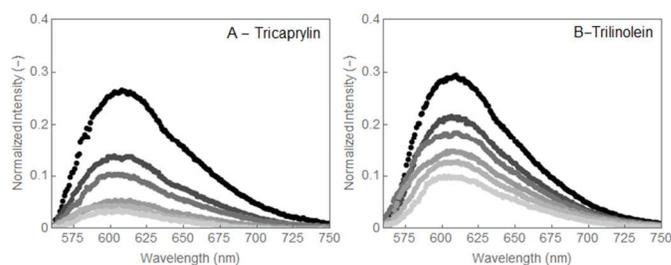

Figure 6. Normalized fluorescence emission spectra of CR in saturated medium chain TAG and tristearin (A) and unsaturated long chain TAG and tristearin (B) solid fat crystal networks. Black: highest proportion of solid fat. Lightest gray: lowest solid fat proportion.

Using the normalized intensities of the emission spectra, which are relative to the viscosity in the microenvironment, it is observed that the viscosity decreases as the solid tristearin content decreases (Figure 7). However, there are no obvious trends that correlate these two parameters. It is not surprising that the confinement of liquid oil is not simply proportional to the solids; numerous other microstructural elements including crystal size, crystal number, distribution, etc. affect the interactions between the continuous oil and solid crystal phases.

In an attempt to better characterize the microstructural elements, polarized light micrographs were obtained for each of the different fat blends (Figure 8). Visually, no obvious differences are observed between blends nor the type of liquid oil. Since no clear trend was initially obvious, microstructural differences were systemically characterized using box-counting fractal dimensions that have been extremely well documented for fat crystal networks.[34, 35] A box-counting fractal dimension, D, is calculated by superimposing grids with side length, l, over a threshold binary image of a fat crystal network with the grids containing particles more than a threshold value being defined as the occupied grids.[36] Early work by Litwinenko et al., has shown that the box-counting fractal dimension is highly sensitive to the space filling colloidal network.[37]
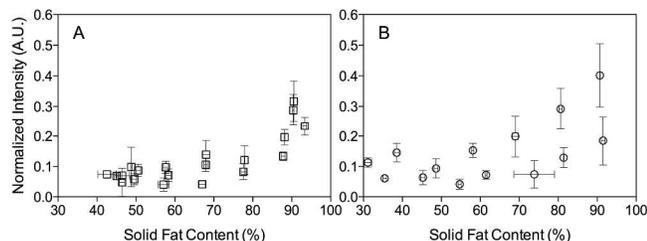

Figure 7. Normalized intensity of CR in each blended fat as a function of the solid fat content in medium chain triglycerides (tricaproin, tricaprylin, and tricaprin) (A) and unsaturated triglycerides (triolein and trilinolein) (B).
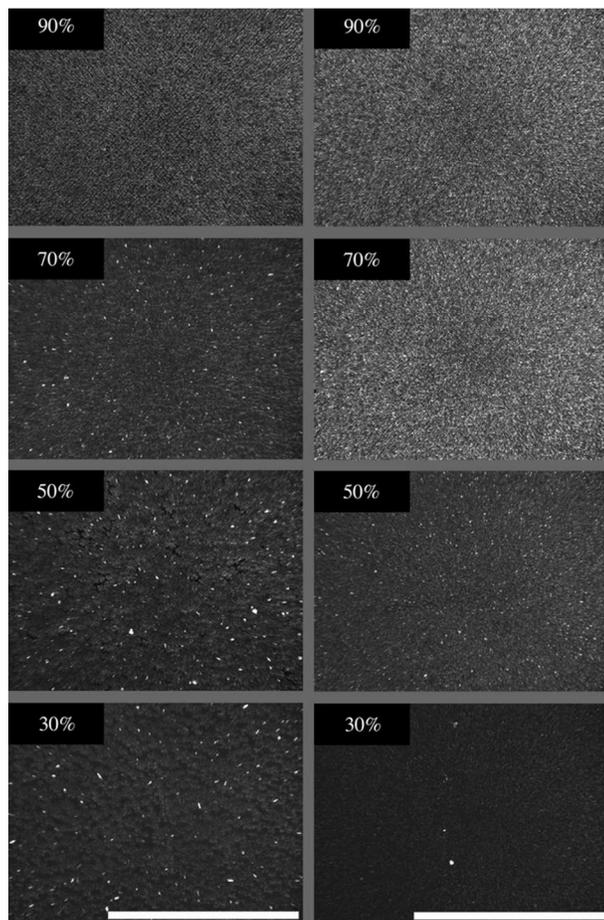

Figure 8: Polarized light micrographs of tristearin blends with different % solids fat contents of tricaprin (left) and triolein (right). The scale bar = 100 μm.

Over small changes in solid fat content there is often a linear correlation with the fractal dimension, however it has been shown that non-linear relationships exist when the solid fat content varies greatly (Figure 9).[38, 39] For medium chain triglycerides, there is a linear relationship with the fractal dimension until approximately 60 % SFC, after which there is a precipitous drop in fractal values (Figure 9A). Also, non-linear relationships between the SFC and fractal dimensions exist for the unsaturated triglycerides (Figure B). Due to the non-linear relationship between these variables, it was believed that the viscosity might preform better as a function of the box-counting fractal dimension.
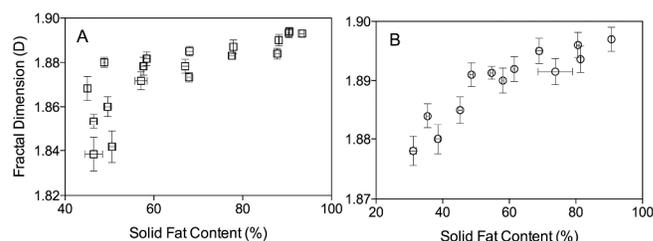

Figure 9: Box-counting fractal dimension in medium chain triglycerides (tricaproin, tricaprylin, and tricaprin) (A) and unsaturated triglycerides (triolein and trilinolein) (B) as a function of solid fat content.

Using the box-counting fractal dimension, a strong log-logistic correlation with the normalized intensity of CR (Y) in the blended fats was observed (Figure 10).

$$Y(x) = a + log\left(1 + e^{(k*(x-c))}\right) \tag{8}$$

where a is the baseline intensity (i.e., viscosity of liquid oil), k is the rate of change of the normalized intensity as a function of the fractal dimension, and c is the critical fractal dimension at which a pronounced change in intensity is observed. Using the parameters obtained from the fits (Table 1), numerous very important insights on the confinement of liquid oil in colloidal fat crystal networks are obtained.
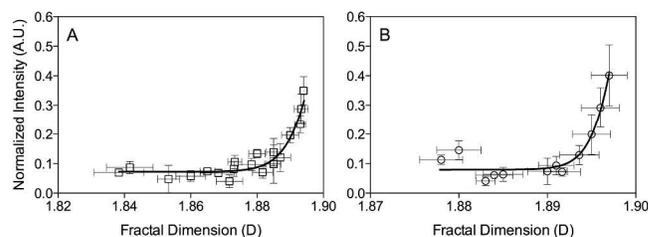

Figure 10: Normalized intensity of CR in each blended fat as a function of the box-counting fractal dimension in medium chain triglycerides (tricaproin, tricaprylin, and tricaprin) (A) and unsaturated triglycerides (triolein and trilinolein) (B).

Table 1: Fitted parameters to the log-logistic fit between the normalized intensity and fractal dimension.

	a	k	c	R²
Medium Chain TAGs	$7.22 \times 10^{-2} \pm 0.71 \times 10^{-2}$	265.3 ± 33	1.896±0.0005	0.81
Unsaturated TAGs	$7.95 \times 10^{-2} \pm 1.00 \times 10^{-2}$	609.7 ± 99	1.897±0.0001	0.82

Of the fitted parameters, the slope, k, and the critical fractal dimension, c, provide two very important insights into understanding liquid oil confinement in colloidal fat crystal networks. Since the data set is normalized, the baseline intensity does not provide significant insights. When the fractal dimension was below 1.89, irrespective of the solvent used, the confinement did not alter the micro-viscosity of the oil. Therefore, when studying oil migration, the effect of confinement may not be significant in low fractal dimension fat blends. However, when the fractal dimension is above 1.89, which is very common, using the viscosity of the bulk liquid oil is likely not representative of the system and as such the micro-viscosity may be an attractive method.

The rate constant, k, for the normalized intensity versus the fractal dimension is much steeper for unsaturated oil (18:1 and 18:2) compared to the medium chain triglycerides (6:0, 8:0 and 10:0). When comparing the k parameters for the unsaturated oil and medium chain triglycerides it is observed that the viscosity as a function of the box-counting fractal dimension increased at a ratio of 2.3:1. As the box-counting fractal dimension increases, the space-filling network also increases which would result in a decrease in the void volume where the liquid oil is confined. It is hypothesised that as the inter-crystal space decreases there will be a greater increase in viscosity for oils with lower molecular volumes. The molecular volumes were predicted using ACD percepta (ACD Inc., Toronto, ON). The average molecular volume for the medium chain triglycerides was 485 cm^3/mol (tricaproin (386 cm^3/mol), tricaprylin (485 cm^3/mol), and tricaprin (584 cm^3/mol)) and for the unsaturated oils 951 cm^3/mol (triolein (961 cm^3/mol) and trilinolein (941 cm^3/mol)). The ratio of the molecular volumes for the unsaturated oils and medium chain triglycerides was 2.3:1, corresponding remarkably well to the ratio of the rate constants. This fluorescence correlation suggests that the oil viscosity at fractal dimension greater than 1.89 will change more for long-chain unsaturated oils compared to the medium chain triglycerides. The sensitivity of a molecular rotor to changes in viscosity is based on steric hindrance of intramolecular rotation, which is related to molecular free volume and molecular crowding around the probe,[17, 32] hence the correlation between fractal dimension and fluorescence intensity.

Conclusions

The use of molecular rotors offers a non-invasive, non-disruptive and highly sensitive alternative to conventional analytical methodologies to evaluate the microenvironment in a fat crystal network. It is clear that the molecular confinement of the oil is dependent on its molecular volume and is strongly dependent on the microstructural elements including the box-counting fractal dimension in high-space filling colloidal fat crystal networks (i.e., D > 1.89). Simply using a bulk oil viscosity may not be appropriate in predicting diffusion of multi-phase materials containing oils as the continuous phase.

Acknowledgements

Notes

[a] School of Environmental and Biological Engineering, Department of Food Science. Rutgers, The State University of New Jersey. 65 Dudley Rd., New Brunswick, NJ, 08901.

* Corresponding author contact information
email address: rogers@aesop.rutgers.edu
ph: 848-932-5520

References

1. J. E. Norton and I. T. Norton, *Soft Matter*, 2010, **6**, 3735-3742.
2. A. G. Marangoni, N. Acevedo, F. Maleky, E. Co, F. Peyronel, G. Mazzanti, B. Quinn and D. Pink, *Soft Matter*, 2012, **8**, 1275-1300.
3. E. Dickinson, *Journal of the Science of Food and Agriculture*, 2013, **93**, 710-721.
4. A. Farhari, Q. Phan and C. Berkland, *Journal of Biomedical Materials Research Part B*, 2014, **102**, 612-618.
5. H.-Y. Ko, J. Park, H. Shin and J. Moon, *Chemistry of Materials*, 2004, **16**, 4212-4215.
6. S. V. Vinogradov and A. V. Kabanov, *Angewandte Chemie International Edition*, 2009, **30**, 5418-5429.
7. E. Dibildox-Alvarado, J. N. Rodrigues, L. A. Gioielli, J. F. Toro-Vazquez and A. G. Marangoni, *Crystal Growth & Design*, 2004, **4**, 731-736.
8. J. Bricknell and R. W. Hartel, *Journal of the American Oil Chemists' Society*, 1998, **75**, 1609-1615.
9. R. Campos and A. G. Marangoni, *Crystal Growth & Design*, 2014, **14**, 1199-1210.
10. F. Maleky, K. L. McCarthy, M. J. McCarthy and A. G. Marangoni, *Journal of Food Science*, 2012, **77**, E74-E79.
11. J. R. Galdamez, K. Szlachetka, J. L. Duda and G. R. Ziegler, *Journal of Food Engineering*, 2009, **92**, 261-268.
12. R. E. Timms, *Confectionery Fats Handbook*, The Oily Press, Bridgwater, England, U.K. , 2003.
13. V. Ghosh, G. R. Ziegler and R. C. Anantheswaran, *Critical Reviews in Food Science and Nutrition*, 2002, **42**, 583–626.
14. L. G. B. Bremer, T. vanVliet and P. Walstra, *Journal fo the Chemical Society: Faraday Transactions*, 1989, **85**, 3359-3372.
15. K. Ichimura, Y. Hayashi, H. Akiyama, T. Ikeda and Ishizuki., *Applied Physical Letters*, 1993, **63**, 449-451.
16. G. S. Kottas, Clarke L.I., D. Horinek and J. Michl, *Chemical Reviews*, 2005, **105**, 1281-1376.
17. M. A. Haidekker and E. A. Theodorakis, *Journal of Biological Engineering*, 2010, **4**, 1-14.
18. B. M. Uzhinov, V. L. Ivanov and M. Ya Melnikov, *Russian Chemical Reviews*, 2011, **80**, 1179 – 1190.
19. R. O. Loutfy and B. A. Arnold, *The Journal of Physical Chemistry*, 1982, 4205-4211.
20. K. Y. Law, *Chemical Physics Letters*, 1980, **75**, 545–549.
21. J. R. Lakowicz, *Principles of Fluorescence Spectroscopy. 3rd Ed.*, Springer Science + Business Media, Baltimore, MD, USA, 2006.
22. N. J. Turro, V. Ramamurthy and J. C. Scaiano, *Modern molecular photochemistry of organic molecules*, University Science Books, Herndon, VA, USA. , 2010.
23. P. B. Mansfield, *Journal of the American Oil Chemists Society*, 1971, **48**, 4-6.
24. F. P. Duval, J. P. M. van Duynhoven and A. Bot, *Journal of the American Oil Chemists Society*, 2006, **83**, 905-912.
25. A. Karperien, NIH, Bethesda, MD, 2007, vol. 2014.

Soft Matter Accepted Manuscript

26.   J. M. Lang, Z. A. Dreger and H. G. Drickamer, *Chemical Physics Letters*, 1995, 78-84.
27.   J. Sutharsan, D. Lichlyter, N. E. Wright, M. Dakanali, M. A. Haidekker and E. A. Theodorakis, *Tetrahedron*, 2010, **66**, 2582–2588.
28.   T. Förster and G. Hoffmann, *Zeitschrift für Physikalische Chemie Neue Folge*, 1971, **75**, 63–76.
29.   L. C. Abbott, S. N. Batchelor, L. Jansen, J. Oakes, J. R. Smith and J. N. Moore, *Journal of Photochemistry and Photobiology A: Chemistry*, 2011, **218**, 11–16.
30.   M. A. Haidekker, T. P. Brady, D. Lichlyter and E. A. Theodorakis, *Bioorganic Chemistry*, 2005, **33**, 415–425.
31.   M. A. J. S. Van Boekel, *Comprehensive Reviews in Food Science and Food Safety*, 2008, **7**, 144-158.
32.   R. W. Sinkeldam, A. J. Wheat, H. Boyaci and Y. Tor, *ChemPhysChem*, 2011, **12**, 567–570.
33.   K. Yasuhara, Y. Sasaki and J. Kikuchi, *Colloids and Surfaces B: Biointerfaces,*, 2008, **67**, 145–149.
34.   D. Tang and A. G. Marangoni, *Journal of the American Oil Chemical Society*, 2006, **83**, 377-388.
35.   D. Tang and A. G. Marangoni, *Journal of the American Oil Chemical Society*, 2006, **83**, 309-314.
36.   D. Tang and A. G. Marangoni, *Advances in Colloid and Interface Science*, 2006, **128-130**, 257-265.
37.   J. W. Litwinenko, A. M. Rojas, L. N. Gerschenson and A. G. Marangoni, *Journal of the American Oil Chemists Society*, 2002, **79**, 647-654.
38.   T. S. Awad, M. A. Rogers and A. G. Marangoni, *Journal of Physical Chemistry B*, 2004, **108**, 171-179.
39.   A. G. Marangoni and M. A. Rogers, *Applied Physics Letters*, 2003, **82**, 3239-3241.

Graphical Abstract

Micro-viscosity of confined oil is not dependent on the solids content, but is dependent on the box-counting fractal dimension in high-space filling colloidal fat crystal networks.